Journal of Thermal Analysis and Calorimetry, Vol. 95 (2009) 1, 21–29

DISSOLUTION KINETIC AND STRUCTURAL BEHAVIOUR OF NATURAL HYDROXYAPATITE *vs*. THERMAL TREATMENT
Comparison to synthetic hydroxyapatite

F. Z. Mezahi[1,2], *H. Oudadesse*[1*], *A. Harabi*[2], *A. Lucas-Girot*[1], *Y. Le Gal*[1], *H. Chaair*[3] *and G. Cathelineau*[1]

[1]Université de Rennes 1, UMR CNRS 6226 Campus Beaulieu, Bâtiment 10B, 35042 Rennes, France
[2]Université de Constantine, Faculté des Sciences, Laboratoire des Céramiques, Constantine, Algérie
[3]Université Hassan II, Faculté des Sciences et Techniques de Mohammedia, Laboratoire de Génie des Procédés, Mohammedia, Maroc

The dissolution kinetic and structural behaviour of natural hydroxyapatite (N-HA) and synthetic hydroxyapatite (S-HA) was studied *vs*. sintering temperature and using 'in vitro' experiments. Obtained results highlight the chemical stability of N-HA. Any structural modification was observed until 1200°C. In the fact S-HA undergoes some modifications. XRD diagrams show the tricalcium phosphate (TCP) phase formation between 800 and 1100°C and tetracalcium phosphate (TetCP) phase formation at 1200°C. The 'in vitro' assay shows that the dissolution was occurred more in N-HA than in S-HA. The formed TCP activated the dissolution kinetic and then the precipitation phenomena when a continuous dissolution of TetCP leaded to slow down the kinetic precipitation.

Keywords: *bone-like apatite, dissolution kinetic, hydroxyapatite, thermal treatment*

Introduction

The bioceramics are widely used for the repair and reconstruction of diseased or damaged parts of the skeleton. They can be used in a variety of shapes and forms: single crystals (sapphire), polycrystalline (alumina or hydroxyapatite (HA)), silicate glass, glass-ceramics and composites (polyethylene-hydroxyapatite) [1–4]. The implanted materials are selected as inert, bioactive, or resorbable materials according to their reaction with living tissue. One of the attractive materials used in clinical field as orthopaedic and dental implants is hydroxyapatite which falls into the categories of bioactive (high density) and resorbable (porous HA) materials. The bioactive materials form a direct biochemical bonds with living tissues. However, the resorbable materials are generally dissolved gradually by the biosystem of the organism and can be replaced by healthy bone without toxicity and rejection [1, 5]. The HA can be prepared from bone or synthesised with several methods, it represents 70 mass% of cortical bone [5]. Nevertheless, synthetic calcium phosphates do no show similar and biological properties as in bone [6]. This is attributed to:

- Differences in chemical composition, which bone contains, in addition to calcium and phosphate, hydrogenophosphate ions, carbonates ions, magnesium, sodium, and numerous other trace elements which play a role in overall performance of human bone.
- The process of resorption of synthetic calcium phosphates which is quite different from that of natural bone, essentially because of different textures [7].

So, hydroxyapatite ceramics manufactured from natural materials such as coral [8] or bone after removal of the organic matter by heating [9, 10] have a widely used for biomedical applications. The 'in vitro' and 'in vivo' studies showed that the natural apatite was well tolerated and has good osteoconductive properties than synthetic HA [11].

The aim of this work is to study the effect of the sintering temperature on the kinetic dissolution of HA. As consequence of the thermal treatment, it will be studying the stability of HA and calcium to phosphorous ratio at any sintering temperature of natural hydroxyapatite prepared from bovine bones and compared the obtained results to the same in the case of use of synthetic hydroxyapatite.

Experimental

In this study, the physico-chemical properties of natural hydroxyapatite granules (N-HA) derived from cortical bovine bones were compared to synthetic hydroxyapatite granules (S-HA) (commercial HA, Alfa: Johnson Matthey Company).

* Author for correspondence: hassane.oudadesse@univ-rennes1.fr

1388–6150/$20.00

Akadémiai Kiadó, Budapest, Hungary
Springer, Dordrecht, The Netherlands

N-HA was obtained by calcination of bone at 800°C during 1 h to remove the organic matter. After that, the calcined bones were dry milled during 30 min.

The different steps of preparation procedure of sintering samples to produce granules are as follows:

- Sieving powders S-HA and N-HA to obtain particles of 60–100 μm.
- Cold compacting under 75 MPa.
- Sintering of compacted powders at different temperatures (800, 900, 1000, 1100, 1200°C) during 2 h.
- Milling and sieving of sintered samples to obtain granules of (200–400 μm).

Several techniques were used to characterise all powders before and after thermal treatment. The existent phases were identified by X-ray diffraction (XRD) technique using Philips PW3710 diffractometer with CuK_α radiation, the calcium to phosphorous molar ratio and ionic concentration of trace elements were determined using inductively coupled plasma-optical emission (ICP-OES) spectrometer. In addition, Fourier transformed infrared spectroscopy (FTIR) was employed to highlight the structural analysis (BRUKER EQUINOX 55). Then, the morphology of granules was studied using scanning electron microscopy (SEM) (JEOL JSM 6301F). However, the density of sintered samples was calculated by direct method using the mass/volume ratio in the samples with 11.5 mm in diameter and 2.3 mm in height.

'In vitro' test were realised by soaking 30 mg of granules into 60 mL of simulated body fluid (SBF) with mineral composition nearly equal to those in human blood plasma at 37°C according to Kokubo protocol [12].

After soaking in SBF at different times (30 min, 3, 6, 9, 12 h, 2, 3.5, 7 days), the granules were filtered, cleaned with ethanol and dried in air. The physico-chemical properties of the filtered granules were studied by FTIR, SEM and ICP-OES in the goal to evaluate the variation of Ca, P, Mg and Na concentrations in SBF with soaking time.

Results and discussion

Physico-chemical characterisation of S-HA and N-HA before thermal treatment

Mineral composition

The ICP-OES technique was used to determine the amount of Ca, P and trace elements like Na, Mg, Sr, Si, K and Zn in S-HA and N-HA powders before thermal treatment (Table 1). These elements present high physiological properties. The molar (Ca/P) ratio was then calculated.

Ca, P concentrations and molar (Ca/P) ratio of N-HA are similar to that of stoichiometric HA (Ca/P=1.67). It contains 40.3% Ca and 18.4% P of mass [13]. However, S-HA have molar (Ca/P) ratio of 1.57. This phosphocalcic ratio is lower than 1.67. It shows that S-HA is deficient hydroxyapatite.

Bone-apatite is characterized by calcium, phosphate and hydroxyl deficiency (molar Ca/P ratio varying from1.37 to 1.87), internal crystal disorder and ionic substitution within the apatite lattice resulting in the presence of significant levels of additional trace elements within bone mineral [14, 15] which play a role in overall performance of human bone [6].

Concerning the trace elements, the two powders have the similar mass% of Na. However, the amount of Mg, Sr, K and Zn in S-HA is lower than that in N-HA. In contrary, S-HA contains Si greater than N-HA. The bone composition differs depending on site, age, dietary history and the presence of disease [16]. Our results of chemical composition of N-HA are in good agreements with that cited in [14, 17–19].

Morphological and structural studies (SEM, XRD and FTIR)

The SEM micrographics of S-HA and N-HA powders before thermal treatment show that S-HA is fine powder; it is formed of agglomerated particles of a needle-like morphology and a size of about 100–500 nm long. However, the N-HA powder is formed with spherical grains of 0.1–1 μm and any longed grains of about 5 μm.

The XRD diagrams of the S-HA and N-HA powders show that all powders are composed of identical phase of hydroxyapatite ($Ca_5(PO_4)_3OH$) (JCDD: file no. 09-0432). The peaks of S-HA are very large in comparison to calcined N-HA. This can be attributed to:

- S-HA is less crystallised than N-HA which was calcined at 800°C to eliminate the organic matter.
- Or, it can contribute the broadening of peaks to the finite size of S-HA crystallite. According to Scherrer equation, the peak width increases when grain size decreases [20].

The FTIR spectra of S-HA and N-HA are presented in Fig. 1. They show that the two powders have much same bands. The absorption bands are summarised in Table 2.

FTIR spectra show the incorporation of CO_3^{2-} ions into hydroxyapatite. There are two sites for inclusion of CO_3^{2-} ions in hydroxyapatite crystals; one in an OH^- site (A-site) and other in a PO_4^{3-} site (B-site) [28, 29].

Besides, bone contains an important quantity of carbonates which can replace the phosphate groups [16]. Bone is not a direct analogue of HA as is

Table 1 Concentrations (mass%) of the principle elements present in S-HA and N-HA powders and the Ca/P molar ratios

	[Ca]	[P]	[Na]	[Mg]	[Sr]	[Zn]	[Si]	[K]	Molar (Ca/P)
S-HA	37.2±0.6	18.3±0.3	0.79	0.29	0.01	0	0.03	0.02	1.57±0.05
N-HA	38.9±0.6	17.9±0.3	0.78	0.59	0.04	0.005	0.01	0.05	1.68±0.05

Table 2 Infrared absorption spectroscopy data for S-HA and N-HA powders

Frequencies/cm^{-1}	S-HA	N-HA	Assignment
PO_4^{3-}	471.7	472.8	doubly degenerated bending mode (ν_2) of the phosphate group [21]
	565.4 603.2	571.2 603.2	triply degenerated bending mode (ν_4) of the O–P–O bond [21]
	962.5	962.2	non-degenerated symmetric stretching mode (ν_1) of the P–O bond of the phosphate group [21]
	1039 1093.2	1057.7 1090.6	triply degenerated asymmetric stretching mode vibration (ν_3) of the P–O bond [22, 23]
		2002.7 2077.1	overtone and combination bands of PO_4^{3-} ions [24]
OH^-	630.6	632.6	liberational mode (ν_L) of the hydroxyl group, OH [23, 24]
	3568.5	3570.4	stretching mode (ν_S) of the hydroxyl group, OH [21, 22]
CO_3^{2-}	874.7	873.7	due to the presence of CO_3^{2-} in OH^- site (A-site) [25] or to HPO_4 characteristic of calcium deficient HA [26]
	1417.6 1456.8	1415.6 1456.9	due to the presence of CO_3^{2-} in site PO_4^{3-} [27]
H_2O	1630 3432	1630 3429.3	adsorbed water [21]
Soluble CO_2	2361.9	2364.2	[21]

commonly believed, but more closely related to an A–B type carbonate-substituted apatite [19, 29] as the same for N-HA in this study.

However, S-HA is characterised by molar ratio (Ca/P) lower than stoichiometric HA which leads to attribute the band at 874.7 cm^{-1} to HPO_4 characteristic of calcium deficient HA [26] and not to presence of CO_3^{2-} in OH^- site.

The analyses of the Infrared bands of S-HA and N-HA confirm that the FTIR spectra of two powders belong to HA. Moreover, in FTIR spectra of N-HA, two weak bands are observed at 3493 and 3540 cm^{-1}. It is possible that these absorptions are due to perturb OH groups that are hydrogen bonded to the halogen anions Cl^- and F^- [30, 31]. The bone can contain small amounts of fluoride (F) and chloride (Cl) which can replace the hydroxyl groups.

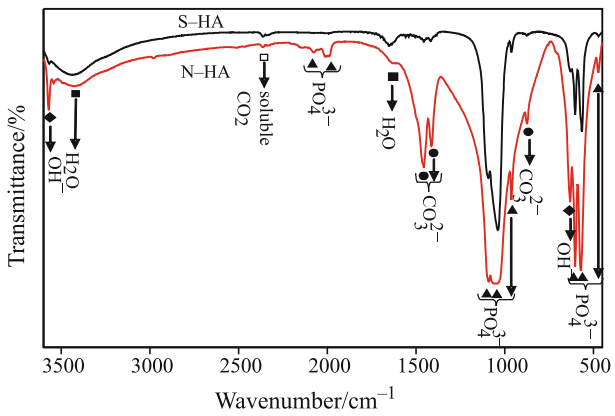

Fig. 1 FTIR spectra of S-HA and N-HA powders before thermal treatment

Physico-chemical characterisation of S-HA and N-HA vs. thermal treatment

The density of samples before and after thermal treatment was calculated by the direct method and illustrated in Fig. 2. The densification starts at 800°C of all compacted powders; then, the rate densification increases when the sintering temperature exceeds 950°C. Besides, we note that the rate of densification for S-HA is very great than that of N-HA. This can be justified by the fact that S-HA has a lower a grain size than N-HA. The use of a fine powder produced a considerable reduction both in the porosity and pore size [32], consequently, the density increases when the grain size decreases.

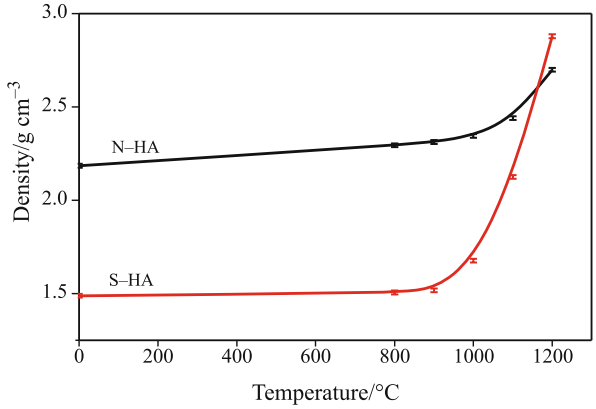

Fig. 2 Density variation of S-HA and N-HA samples with sintering temperature

Mineral composition modifications

The effect of increasing sintering temperature in the stability of initial phases and consequently the change of molar (Ca/P) ratio with thermal treatment was evaluated. For S-HA, the sintering temperature affects the molar ratio which changes from 1.57 before thermal treatment to 1.61–1.63 after thermal treatment. This change is related to the formation of new phases caused by decomposition of HA to tricalcium phosphate or tetracalcium phosphate as is demonstrated by XRD results (Fig. 4). However, the (Ca/P) remains constant in N-HA when the sintering temperature increases. This confirms that no new phase was formed in sintered granules of N-HA.

Morphological and structural studies: (SEM, XRD and FTIR)

The SEM micrographics of sintered granules (Fig. 3) are in a good agreement with obtained results of density. The porosity decreases and grain size increases when the sintering temperature increases of all compounds. Effectively, at 1200°C, it is difficult to distinguish the grain boundaries especially in S-HA compounds. Consequently, the pores size observed in S-HA compounds are lower than that in N-HA compounds. The calcination leads to more rounded particles and to formation of necks between these particles. The coalescence of particles is more important when (Ca/P) decreases [26] and compacted powders are very fine [32].

In this part, we present only the physico-chemical properties of granules sintered at 800, 1100 and 1200°C. For samples sintered at 900 and 1000°C; their physico-chemical properties have the same variation as samples sintered at 800°C.

Heat treatment of S-HA produced several modifications in the XRD patterns (Fig. 4, S-HA):

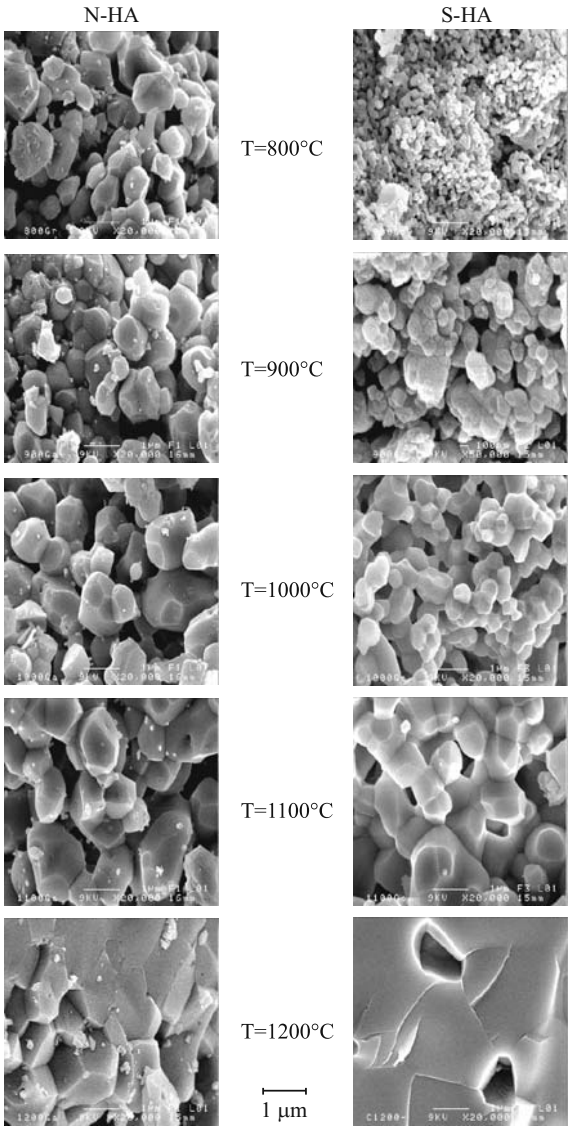

Fig. 3 SEM micrographs of N-HA and S-HA samples, sintered at different temperatures

- From 800 to 1000°C, a minor new phase was formed which it is result of partial decomposition of HA to β-tricalcium phosphate ($Ca_3P_2O_8$) (β-TCP).
- At 1100°C, more β-TCP was formed in addition to apparition of α-TCP as minor phase.
- However, at 1200°C, the XRD pattern shows apparition of tetra-calcium phosphate (TetCP): ($Ca_4P_2O_9$), it has been reported that TetCP and HA have similarities in their X-ray diffraction patterns and the two salts are structurally related [33, 34]. This makes difficulties to detect TetCP in the presence of HA. This difficulty is compounded by the fact that the indexes of refraction of TetCP and HA are close to each other and the IR spectrum has no strong peaks that distinguish it in the presence of HA [23]. Consequently, the peaks of two phases are very near.

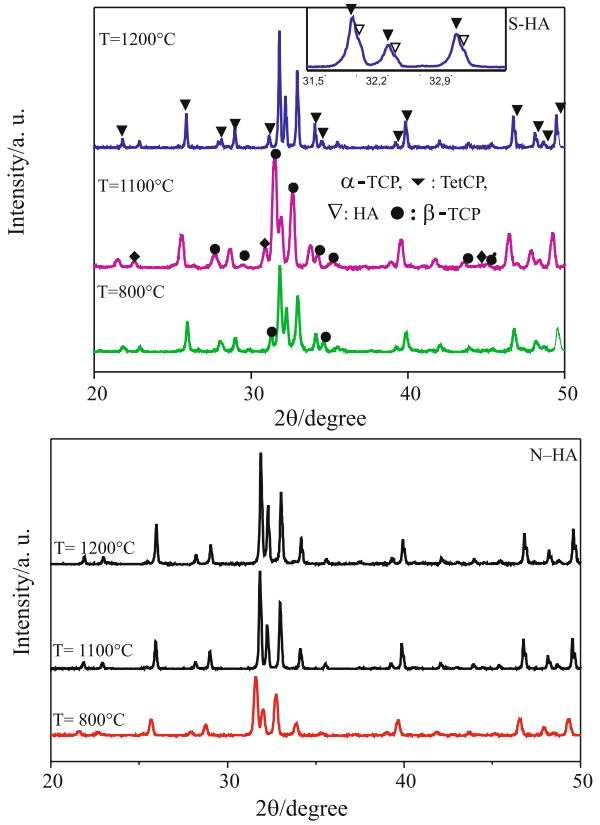

Fig. 4 XRD diagrams of S-HA and N-HA granules, sintered at different temperatures

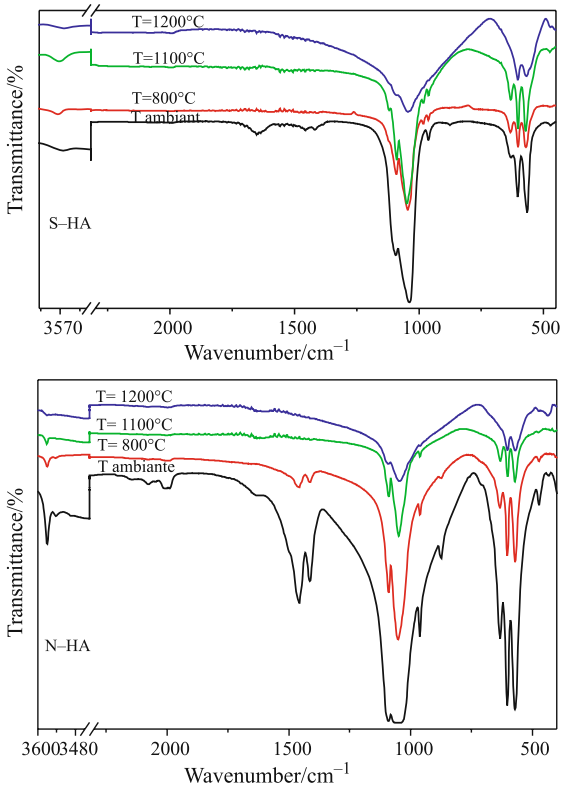

Fig. 5 FTIR spectra of S-HA and N-HA granules, sintered at different temperatures

HA was decomposed to major phases TCP and TetCP and a minor phase CaO (2θ=37.37°).

However, no difference among the all XRD patterns of N-HA (Fig. 4, N-HA) was observed, and no additional phase was identified. This indicates that the sintering process has not modified the composition of N-HA. At ambient temperature, the presence of the fluoride in the initial HA induces a shift of the XRD pattern [35].

The thermal treatment has led to an alteration structural of sintered S-HA as shown in Fig. 5. The FTIR of sintered granules of S-HA (Fig. 5, S-HA) shows the elimination of carbonate groups after sintering since 800°C and for all temperatures. Besides, the bands intensities of OH^- groups decrease with temperature. In addition, new phases were formed after thermal treatment as demonstrated by apparition of new bands:

- New bands appeared in FTIR spectra of granules S-HA sintered at temperature varying from 800 to 1100°C; a band at 1121 cm^{-1} corresponding to one of the characteristic stretching of tetrahedral of PO_4^{3-} band groups of β-TCP [36] and a band at 981 cm^{-1} correspond to α-TCP [37]. It can be noted that it is difficult to distinguish between both crystalline phases of TCP, since both α-TCP and β-TCP exhibit several bands at similar wave numbers [36]. α-TCP was not observed in XR diagrams of S-HA/800, 900 and 1000°C although the apparition of their band in FTIR spectra. This is probably that a minor phase α-TCP was formed.
- Moreover, in FTIR spectrum of S-HA/1200°C, the OH^- band at 631 cm^{-1} is eliminated and the band at 3571 cm^{-1} is very weak as consequence of the formation of new phases as shown in DRX spectra (Fig. 7, S-HA/1200°C). So, new bands appeared at 1012 and 1117 cm^{-1} characteristic of PO_4^{3-} band groups of TetCP [23, 38] which has led to broadening of band centred at 1046 cm^{-1}. The weak band at 3571 cm^{-1} affirms the presence of HA in sintered granules S-HA at 1200°C.

FTIR spectra of sintered granules of N-HA is similar (Fig. 5, N-HA) of the same powder before sintering. The observed differences are:

- Decrease of the intensities bands of carbonate and OH^{-1} groups when sintering temperature increases.
- Elimination of carbonate and hydrogen bonded to the halogen anions from the apatite's structure at 1100 and 1200°C. The results of FTIR confirm that no new phase occurred during the thermal treatment of N-HA.

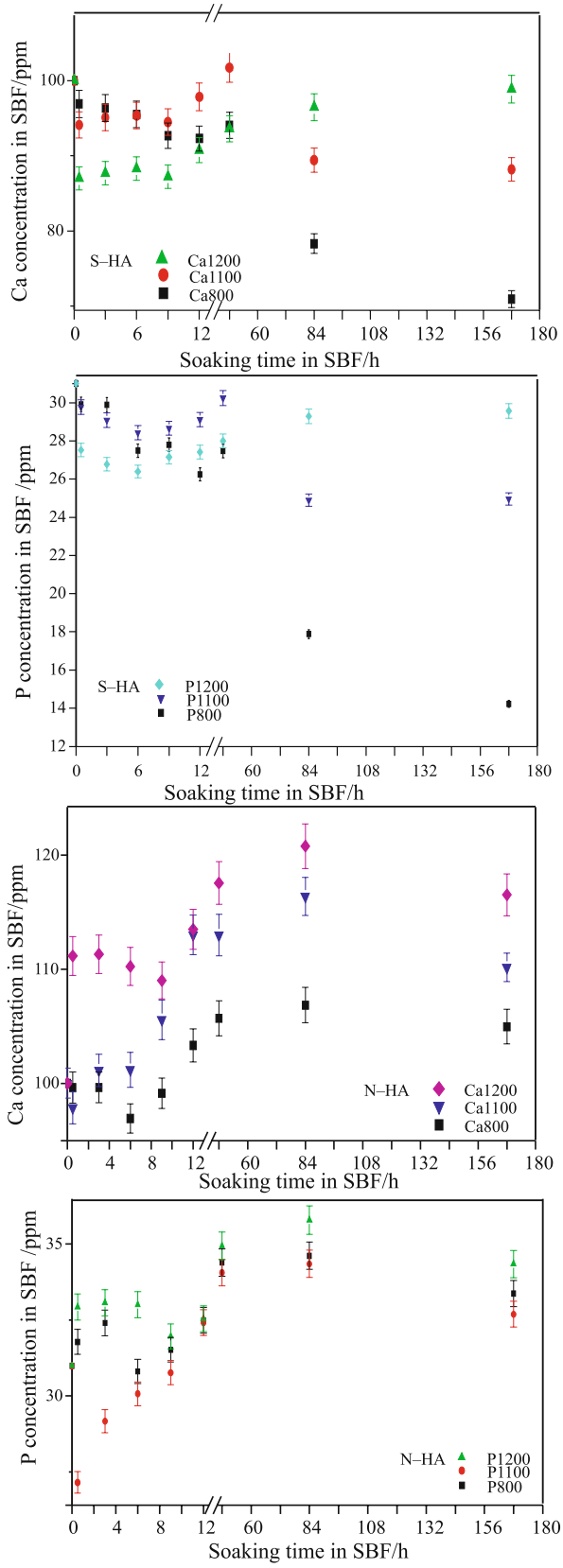

Fig. 6 Variations of Ca and P concentrations in the SBF solution *vs*. soaking time

'In vitro' experiments

Variation of Ca, P, Mg and Na concentration in SBF with soaking time

The variations of calcium and phosphorous ions concentrations in SBF as a function of soaking time, evaluated with ICP-OES method, are shown in Fig. 6.

For all sintering temperatures of S-HA, a decrease of Ca and P concentration after 30 min soaking in SBF was occurred. After 30 min soaking time, the variation of Ca and P concentration is as follows:

- For S-HA/800°C, Ca and P concentration in SBF decreases with increase of soaking time until 7 days.
- However for S-HA/1100°C, after 30 min, Ca and P concentration remains constant until 9 h, then it increases to reach maximum after 2 days soaking in SBF. Afterwards, it decreases and remains constant. This phenomenon corresponds to precipitation process of bone like apatite on the surface of S-HA granules sintered at $T \leq 1100$°C.
- In contrary, for S-HA/1200°, after 30 min of exposition to SBF, the Ca and P concentration increases with soaking time which indicates the dissolution of tetra-calcium phosphate. The decomposition products of HA dissolve more rapidly in the body fluid than crystalline HA, in the following order: CaO>>TTCP>TCP>>HA [39]. This continuous dissolution will be inhibiting the precipitation process of bone-like apatite as demonstrate by SEM and FTIR analysis.

For short soaking time (30 min) of N-HA granules in SBF, the Ca and P concentration increases when sintering temperature increases, this is result of intense calcium dissolution which predominates over the precipitation of the new phosphate phases. The kinetic process of dissolution-precipitation of the N-HA for all temperatures is as follows:

- After 30 min, slowly increase of Ca and P in SBF was occurred; the calcium phosphate precipitation equilibrates the calcium phosphate dissolution. Than, a higher increase of Ca and P concentration in SBF as consequence of predomination of dissolution than precipitation of the new calcium phosphate. Afterwards, the precipitation of new phosphate phase dominates the dissolution-precipitation kinetic. Ca and P dissolution was higher after 3.5 days of soaking time in SBF of sintered granules.
- The increase of Ca and P ion concentrations is due to the ionic exchange between H^+ within the SBF solution and Ca^{2+} in HA. After maximum point reaching, a decrease of Ca and P ions concentration is occurred which suggesting a continuous precipitation of the bone-like apatite layer [40].

According to Kim-theory, the negative surface of HA attracts the Ca ions in SBF solution to form the Ca-rich amorphous calcium-phosphate (ACP). After immersion in SBF, HA is characterised by a negative surface as consequence of exposing their hydroxyl and phosphate units. The second step, the phosphate ions in the SBF interact with Ca-rich ACP to form Ca-poor ACP. Finally the Ca-poor ACP crystallises gradually into bone-like apatite and HA stabilises their surface in SBF [41].

It was observed that the concentrations of Mg and Na ions have the same variation in SBF solution as Ca and P for the N-HA and S-HA. After reaching maximum dissolution, Mg and Na ions will be incorporated into bone-like apatite [38]. We conclude that Mg and Na play a complementary role to that of Ca [42]. Ca is major element and presents a high interest in the bony calcification when Mg advantages the biological hydroxyapatite formation and inhibits action on the calcification mechanism, particularly in presence of Na and Sr.

SEM and FTIR analysis of immerged granules

The SEM images of immerged granules at 7 days are shown in Fig. 7. For S-HA, sintering temperatures varying from 800 to 1100°C show the uniform layer of calcium phosphate.

- The bone-like apatite was formed in S-HA/800°C especially inside the pore cavities, it was not very dense. In this case, the supersaturation was achieved inside the pores and consequently the precipitation process occurred between grains.
- However, in S-HA/1100°C, all the grains were covered by the bone-like apatite. The presence of soluble phase such as TCP promotes the formation of bone-like apatite [43].
- But, in S-HA/1200°C granules, no the bone-like apatite was formed. This result can be explained by the fact that the formation of TetCP has led to a continuous dissolution of sintered granules at 1200°C. It is in good agreement with variation of Ca concentration in SBF of S-HA/1200°C granules, if the rate of dissolution is accelerated, the precipitation process is delayed. The same result was obtained in Monteiro's works [43]. The sintered β-tricalcium phosphate exhibited a poor ability of inducing Ca-P formation both 'in vitro' and 'in vivo'. So, it is like better to use the biphasic ceramics composed of HA and TCP or HA and TetCP than use pure HA or pure resorbable phases (TCP, TetCP).

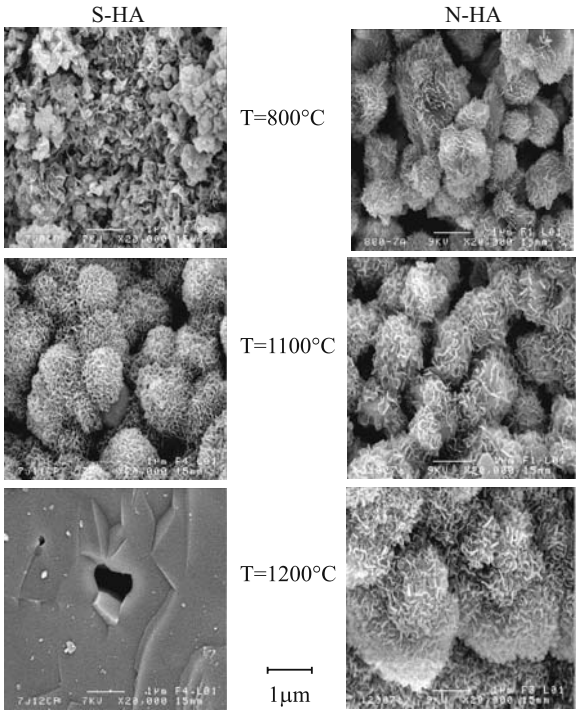

Fig. 7 SEM images of S-HA and N-HA granules soaked in SBF for 7 days

However, in N-HA, the calcium phosphate was formed at surface of granules sintered at any temperatures, above all the grains sintered at 1200°C; the grains were totally covered by thick layer of bone like apatite as shown in Fig. 7.

The infrared spectra (Fig. 8) have confirmed the ICP-OES and SEM results. For S-HA, they show that only for sintering temperatures varying from 800 to 1100°C, an increase of band intensity of phosphate and hydroxyl bands was increased and a weak band of carbonate was observed. However, they show that N-HA exhibit highest efficiency in phosphate layers formation, an increase of band intensity of OH^{-1} at 630 and 3570 cm^{-1} after 7 days of soaking into SBF. This confirms the apatite formation, associated with carbonates for all temperatures (at 1200°C, the intensity of carbonate band is very weak) after immersion in SBF.

By comparison of all result after immersion of S-HA and N-HA granules, it can be observed that a formation of bone like apatite is much related to the existent phases at any sintering temperature. The formation of TCP during sintering favourites the formation of bone-like apatite, however the TetCP is undesirable because of their high solubility in SBF. These results are in good agreement with the Monteiro studies [43], they have shown that a minor phase such as TCP contribute to the dissolution of the granules and to the precipitation of the bone-like apatite. Than, the exposition of biphasic (HA/TCP) to medium culture leads to precipitation of a bone-like apatite more than pure TCP or pure HA [44, 45].

In the case of immerged granules of N-HA, the following phenomena were observed:

- The dissolution kinetic increases with the sintering temperature.

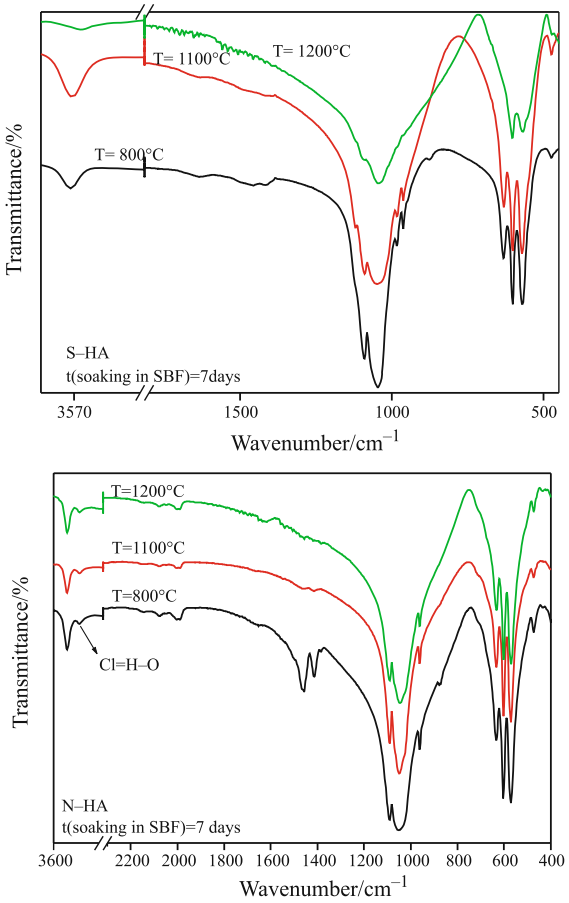

Fig. 8 FTIR spectra of S-HA and N-HA granules soaked in SBF for 7 days

- The new phosphate phase was formed with higher thick on the surface of granules sintered at higher temperatures.
- The new phase precipitate was associated with carbonated (bone-like) apatite.

The bone is recognised by its internal crystal disorder and ionic substitution within the apatite lattice resulting in the presence of significant levels of chloride and fluoride and it is more closely related to an A–B type carbonate-substituted apatite [19, 32]. These factors all contribute to an apatite that is insoluble enough for stability [46]. The substitution of fluoride in bone decreases its dissolution such as in teeth [47, 48]. Besides, the low [OH^-] in the bone apatite would enable its dissolution. It is recognised that if the dissolution rate of calcium phosphate ceramics is increased, the precipitation of biologically equivalent apatite in SBF is enhanced [43]. The FTIR spectra of the sintered granules show that fluoride and chloride intensity bands decrease with sintering temperature in N-HA. Consequently, the dissolution and precipitation process increases with temperature [49, 50].

The comparison of kinetic dissolution of Ca and P shows that maximum value of dissolution in S-HA is less than in N-HA. Consequently the precipitation of new phosphate phase is more in N-HA despite that S-HA have molar ratio (Ca/P) lower than N-HA. This is due to the presence of Mg, Sr and Zn in N-HA with concentration higher to that in S-HA. The inclusion of these ions such as carbonate, sodium and trace levels of silicon and zinc within the apatite lattice has thus been postulated to improve the bioactivity of the material [7, 46].

Conclusions

The purpose of this work is studying the kinetic dissolution *vs*. thermal treatment of natural hydroxyapatite and comparison with synthetic hydroxyapatite. The experimental results have shown that dissolution kinetic of N-HA increases with the sintering temperature. Consequently, the new phosphate phase was formed with higher thick as observed in Fig. 7 on the surface of granules sintered at higher temperatures.

However, in S-HA, the formation of bone like apatite is very sensitive to phase's existent at any sintering temperature. The formation of TCP favours the formation of new phase. Conversely, the continuous dissolution of tetracalcium phosphate (TetCP) is unfavourable to precipitation of the calcium phosphate.

The dissolution was occurred more in N-HA that in S-HA and consequently the precipitation of new phosphate phase is more in N-HA.

Different factors such as Ca/P molar ratio, trace elements, and sintering temperature affect the density, the chemical composition and then the dissolution and the precipitation processes of HA. Origin of HA; trace elements and sintering temperature have an important effect on the formation of bone-like apatite.

References

1 L. L. Hench, J. Am. Ceram. Soc., 74 (1991) 1487.
2 H. Oudadesse, A. C. Derrien, S. Martin, A. Lucas-Girot and G. Cathelineau, Biomed. Mater., 2 (2007) 65.
3 H. Oudadesse and A. C. Derrien, J. Therm. Anal. Cal., 82 (2005) 323.
4 M. Ciecinka, J. Therm. Anal. Cal., 72 (2003) 199.
5 V. A. Dubok, Powd. Metall. Metal Ceram., 39 (2000) 7.
6 D. Shi, Biomaterials and Tissue Engineering, Springer Berlin Heidelberg, New York 2004, p. 2.
7 R. Lanza, R. Langer and W. Chick, Principles of Tissue Engineering, Academic Press Inc., San Diego CA 1997, p. 603.
8 D. Roy and S. K. Linnehan, Nature, 247 (1974) 220.
9 K. A. Hing, S. M Best, K. E. Tanner, W. Bonfield and P.A. Revell, J. Mater. Sci., 10 (1999) 663.
10 S. Joschek, B. Nies, R. Krotz and A. Goepferich, Biomaterials, 21 (2000) 1645.
11 S. Guizzardi, J. Biomed. Mater. Res., (2000) 53.

12 T. Kokubo, H. Hushitani, S. Sakka and S. T. Yamamuro, J. Biomed. Mater. Res., 24 (1990) 721.
13 R. G. V. Hancock., M. D. Grynpas and B. Alpert, J. Radioanal. Nucl. Chem., 110 (1987) 283.
14 D. McConnell, Apatite, Springer Verlag, Vienna–Heidelberg–New York 1973, p. 111.
15 A. S. Posner, Physiol. Rev., 49 (1969) 760.
16 N. K. Aras, G. Yiimaz, S. Alkan and F. Korkusuz, J. Radioanal. Nucl. Chem., 239 (1999) 79.
17 F. C. M Driessens, Bull. Soc. Chim. Belg., 89 (1980) 663.
18 H. Aoki, Science and Medical Applications of Hydroxyapatite, Takayama Press System Centre, Tokyo 1991, p. 165.
19 R. Z. Le Geros and J. P. Le Geros, In an Introduction to Bioceramics, World Scientific 1993, p. 39.
20 B. D. Cullity, Elements of X-ray Diffraction, Addison-Wesley 1978, p. 100.
21 S. Koutsopoulos, J. Biomed. Mater. Res., 62 (2002) 600.
22 I. Rehman and W. Bonfield, J. Mater. Sci., 8 (1997) 1.
23 Y. Sargin, M. Kizilyalli, C. Telli and H. Güler, J. Eur. Ceram. Soc., 17 (1997) 963.
24 S. J. Joris and C. H. Amberg, J. Phys. Chem., 75 (1971) 3172.
25 H. R. Ramay and M. Zhang, Biomaterials, 24 (2003) 3293.
26 S. Raynaud, E. Champion, D. Bernache-Assollant and P. Thomas, Biomaterials, 23 (2002) 1065.
27 M. Vignoles, G. Bonel, D. W. Holcomb and R. A. Young, Calcif. Tissue Int., 45 (1989) 157.
28 A. L. Underwood, T. Y. Toribara and W. F. Neuman, J. Am. Chem. Soc., 77 (1955) 317.
29 J. B. Elliot, Structure and Chemistry of the Apatites and other Calcium Orthophosphates, Elsevier, Amsterdam 1994, p. 161.
30 H. J. Allan, British Division of the International Association for Dental Research, British Division 1969, p. 1095.
31 H.-W. Kim, Y.-J. Noh, Y.-H. Koh, H.-Ee Kim and H.-M. Kim, Biomaterials, 23 (2002) 4113.
32 A. Almirall, M. P. Ginebra, G. Larrecq, J. A. Delgado, S. Martinez and J. A. Planell, Biomaterials, 25 (2004) 3671.
33 W. E. Brown and E. P. Epstein, J. Res. Nat. Bur. Stand., 69A (1965) 547.
34 B. Dickens, W. E. Brown, G. J. Kruger and J. M. Etewart, Acta Cryst., B29 (1973) 2046.
35 J. C. Rendon-Angeles, K. Yanagisawa, N. Ishizawa and S. Oishi, Chem. Mater., 12 (2000) 2143.
36 S. Habelitz, L. Pascal and A. Duran, J. Mater. Sci., 36 (2001) 4131.
37 A. Jillavenkatesa and R. A. Condrate, Spec. Lett., 31 (1998) 1619.
38 U. Posset, E. Löcklin, R. Thull and W. Kiefer, J. Biomed. Mater. Res., 40 (1998) 640.
39 C. P. A. T. Klein, Biomaterials, 11 (1990) 509.
40 Y. W. Gua, K. A. Khora and P. Cheang, Biomaterials, 25 (2004) 4127.
41 H.-M. Kim, T. Himeno, T. Kokubo and T. Nakamura, Biomaterials, 26 (2005) 4366.
42 H. Oudadesse, A. C. Derrien, M. Lefloch and J. Davidovits. J. Mater. Sci., 42 (2007) 3092.
43 M. M. Monteiro, N. C. C. da Rocha, A. M. Rossi and G. de A. Soares, J. Biomed. Mater. Res., 65A (2003) 299.
44 R. Xin, Y. Leng, J. Chen and Q. Zhang, Biomaterials, 26 (2005) 6477.
45 J.-M. Bouler and G. Daculsi, Key Eng. Mater., 192–195 (2001)119.
46 K. A. Hing, Phil. Trans. R. Soc. Lond. A, 362 (2004) 2821.
47 J. D. Pasteris, B. Wopenka, J. J. Freeman, K. Rogers, E. V.-Jones, J. A. M. V. D. Houwen and M. J. Silva, Biomaterials, 25 (2004) 229.
48 W. Suchanek, M. Yashima, M. Kakihana and M. Yoshimura, Biomoterials, 18 (1997) 923.
49 G. C. Koumoulidis, C. C. Trapalis and T. C. Vaimakis, J. Therm. Anal. Cal., 84, (2006) 165.
50 A. Bianco, I. Cacciotti, M. Lombardi, L. Montanaro and G. Gusmano, J. Therm. Anal. Cal., 88 (2007) 237.

Received: February 19, 2008
Accepted: April 15, 2008
OnlineFirst: September 20, 2008

DOI: 10.1007/s10973-008-9065-4